

Combined effects of thermal radiation and Hall current on MHD free-convective flow and mass transfer over a stretching sheet with variable viscosity

G. C. Shit* and R. Haldar

Department of Mathematics

Jadavpur University, Kolkata - 700032, India

Abstract

An analysis has been investigated for the effects of thermal radiation and Hall current on magnetohydrodynamic free-convective flow and mass transfer over a stretching sheet with variable viscosity in the presence of heat generation/absorption. The fluid viscosity is assumed to vary as an inverse linear function of temperature. The boundary-layer equations governing the flow problem under consideration have been reduced to a system of non-linear ordinary differential equations by employing a similarity transformation. Using the finite difference scheme, numerical solutions to the transform ordinary differential equations have been solved and the results that obtained are presented graphically. With an aim to test the accuracy, the numerical results have been compared with the existing scientific literature and found excellent agreement.

Keywords: Thermal radiation; Variable viscosity; MHD; Hall current; Heat and Mass transfer

1 Introduction

In the recent past there has been a growing interest in boundary-layer flow on a continuous moving surface in the presence of magnetic field with or without considering the effect of Hall

*Email address: gcs@math.jdvu.ac.in (G. C. Shit)

current. But, of course these are very significant type of flow towards the several engineering applications, such as in polymer processing, electro-chemistry, MHD power generators, flight magnetohydrodynamics as well as in the field of planetary magnetosphere, aeronautics and chemical engineering.

Sakiadis [1] first explored the study of boundary-layer flow on a continuous moving surface and Crane [2] extended this problem to a stretching sheet whose surface velocity varies linearly with the distance x from a fixed origin. During the past decades several investigators [3-10] have considered the boundary-layer flow problems under different physical situations. Gupta and Gupta [11] examined the heat and mass transfer over a stretching sheet subject to suction or blowing. The influence of a uniform magnetic field on the flow of an electrically conducting fluid past a stretching sheet was investigated by Pavlov [12], Andersson [13], Andersson et al.[14], Gupta and Chakrabarty [15], Char [16], Watanabe and Pop [17] and Elbashbeshy [18]. The chemical reaction on free-convective flow and mass transfer of a viscous, incompressible and electrically conducting fluid over a stretching sheet was investigated by Afify [19] in the presence of a uniform transfer magnetic field. In all these investigations the electrical conductivity of the fluid was assumed to be uniform and low magnetic field intensity. However, in an ionized fluid where the density is low and thereby magnetic field intensity is very strong, the conductivity normal to the magnetic field is reduced due to the spiraling of electrons and ions about the magnetic lines of force before collisions take place and a current induced in a direction normal to both the electric and magnetic fields. This phenomena is known as Hall effect. Watanabe and Pop [20] investigated the magnetohydrodynamic boundary-layer flow over a continuously moving semi-infinite flat plate by taking into account the Hall currents. Aboeldahab [21] and Aboeldahab and Elbarbary [22] studied the Hall current effects on MHD free-convective flow past a vertical plate with mass transfer. Shit [23] investigated the Hall effects on MHD free-convective flow and mass transfer over a stretching sheet in the presence of chemical reaction. Fakhar et al. [24] studied the Hall effects on the unsteady magnetohydrodynamic flow of a third grade fluid without considering the heat and mass transfer phenomena. The effect of Hall currents on the steady MHD flow of Berger's fluid between two parallel electrically insulating infinite planes was carried out by Rana et al. [25].

Recently, a new idea is added to the study of boundary-layer fluid flow and heat transfer is the consideration of the effect of thermal radiation and temperature dependent viscosity. Many processes in engineering applications occur at high temperatures and the radiate heat transfer becomes very important for the design of the pertinent equipment. In view of this, Rapits and Perdakis [26] and Rapits [27] studied respectively the flow of a visco-elastic fluid and micropolar fluid past a stretching sheet in the presence of thermal radiation. Mukhopadhaya et al. [28] investigated the problem of MHD boundary-layer flow over a heated stretching sheet with variable viscosity. The radiation effect on boundary-layer flow with or without applying magnetic field under different situations were studied by Shateyi [29], Mahmoud [30], Pal and Talukdar [31] and Pal and Chatterjee [32]. However, Salem [33] investigated the effect of variable viscosity on MHD viscoelastic fluid flow and heat transfer over a stretching sheet without considering thermal radiation effect. Shit and Haldar [34] carried out the study of the effect of thermal radiation on MHD viscoelastic fluid flow past a stretching surface with variable viscosity. But, no attempt is available in the existing scientific literatures for the consideration of the combined effect of thermal radiation and Hall current on the study of MHD boundary-layer flow. Thus the present study fills the gap in this directions.

Again, combined heat and mass transfer problems with chemical reaction are of increasing importance in many processes, like drying, evaporation at the surface of a water body, energy transfer in a wet cooling tower etc. In this context, Muthucumarswamy and Ganesan [35] studied the effect of the chemical reaction and injection as well as flow characteristics in an unsteady upward motion of an isothermal plate. Chamakha [36] carried out the MHD flow of uniformly stretching vertical permeable surface in the presence of heat generation / absorption along with the chemical reaction. Very recently, Mohamed and Abo-Dahab [37] have investigated the influence of chemical reaction and thermal radiation on hydromagnetic free-convective heat and mass transfer for a micropolar fluid via a porous medium bounded by an infinite vertical porous plate in the presence of heat generation. Seddeek et al. [38, 39] analyzed the effects of chemical reaction, radiation and variable viscosity on hydromagnetic mixed convection heat and mass transfer. In all these studies ignores the effect of the consideration of Hall current.

Now we propose to study the combined effects of thermal radiation and Hall current on

the hydromagnetic free-convective flow and mass transfer over a stretching surface with variable viscosity in the presence of heat generation/absorption. The present problem pertains to situation in which the n -th order chemical reaction takes place. Thus the study is also applicable to the elongation of the bubbles and in bioengineering where the flexible surfaces of the biological cells and membranes in living systems are typically surrounded with fluids which are electrically conducting and being stretched constantly.

2 Mathematical Formulation

We consider the steady free-convective flow and mass transfer of an incompressible, viscous and electrically conducting fluid past a stretching sheet and the sheet is stretched with a velocity proportional to the distance from a fixed origin O (cf. Fig. 1). A uniform strong magnetic field of strength B_0 is imposed along the y -axis and the effect of Hall currents is taken into account. Taking Hall effects into account the generalized Ohm's law [40] may be put in the form :

$$\vec{J} = \frac{\sigma}{1 + m^2} \left(\vec{E} + \vec{V} \times \vec{B} - \frac{1}{en_e} \vec{J} \times \vec{B} \right),$$

where \vec{V} represents the velocity vector, \vec{E} is the intensity vector of the electric field, \vec{B} is the magnetic induction vector, ν_e the magnetic permeability, \vec{J} the electric current density vector, $m = \frac{\sigma B_0}{en_e}$ is the Hall current parameter, σ the electrical conductivity, e the charge of the electron and n_e is the number density of the electron. A very interesting is that effect of Hall current gives rise to a force in the z -direction which in turn produces a cross flow velocity in this direction and thus the flow becomes three-dimensional.

The temperature and the species concentration are maintained at a prescribed constant values T_w, C_w at the sheet and T_∞ and C_∞ are the fixed values far away from the sheet. Since the concentration of diffusing species is very small in comparison to other chemical species, the Soret and Dufour effects are neglected.

Following Lai and Kulacki [41], the fluid viscosity μ is assumed to vary as a reciprocal of a linear function of temperature given by

$$\frac{1}{\mu} = \frac{1}{\mu_\infty} [1 + \gamma(T - T_\infty)] \quad (1)$$

or

$$\frac{1}{\mu_\infty} = a(T - T_r) \quad (2)$$

where $a = \frac{\gamma}{\mu_\infty}$ and $T_r = T_\infty - \frac{1}{\gamma}$.

In the above equation both a and T_r are constants, and their values depend on the thermal property of the fluid, i.e., γ . In general $a > 0$ represent for liquids, whereas for gases $a < 0$.

By assuming Rosseland approximation for radiation, the radiative heat flux q_r is given by

$$q_r = -\frac{4\sigma^*}{3K} \frac{\partial T^4}{\partial y} \quad (3)$$

where σ^* is the Stefan-Boltzman constant and K the mean absorption coefficient. We assume that the temperature differences within the flow are sufficiently small such that T^4 may be expressed as a linear function of the temperature as shown in Chamakha [36]. Expanding T^4 in a Taylor series about T_∞ and neglecting higher order terms, we obtain

$$T^4 \cong 4T_\infty^3 T - 3T_\infty^4 \quad (4)$$

Substituting T^4 from (4) in (3) and differentiating the resulting equation with respect to y , we obtain as

$$\frac{\partial q_r}{\partial y} = -\frac{16\sigma^* T_\infty^3}{3K} \frac{\partial^2 T}{\partial y^2} \quad (5)$$

Owing to the above mentioned assumptions, the boundary layer free-convection flow with mass transfer and generalized Ohm's law is governed by the following system of equations :

$$\frac{\partial u}{\partial x} + \frac{\partial v}{\partial y} = 0, \quad (6)$$

$$\begin{aligned} \rho_\infty \left(u \frac{\partial u}{\partial x} + v \frac{\partial u}{\partial y} \right) = \frac{\partial}{\partial y} \left(\mu \frac{\partial u}{\partial y} \right) + \rho_\infty g \beta_t (T - T_\infty) + \rho_\infty g \beta_c (C - C_\infty) \\ - \frac{\sigma B_0^2}{1 + m^2} (u + mw), \end{aligned} \quad (7)$$

$$\rho_{\infty} \left(u \frac{\partial w}{\partial x} + v \frac{\partial w}{\partial y} \right) = \frac{\partial}{\partial y} \left(\mu \frac{\partial w}{\partial y} \right) + \frac{\sigma B_0^2}{1 + m^2} (mu - w), \quad (8)$$

$$\rho_{\infty} c_p \left(u \frac{\partial T}{\partial x} + v \frac{\partial T}{\partial y} \right) = k \frac{\partial^2 T}{\partial y^2} - Q (T - T_{\infty}) - \frac{\partial q_r}{\partial y}, \quad (9)$$

$$u \frac{\partial C}{\partial x} + v \frac{\partial C}{\partial y} = D \frac{\partial^2 C}{\partial y^2} - k_0 (C - C_{\infty})^n, \quad (10)$$

where (u, v, w) are the velocity components along the (x, y, z) directions respectively, μ is the coefficient of viscosity, g the acceleration due to gravity, β_t the coefficient of thermal expansion, β_c the coefficient of expansion with concentration, T and C are the temperature and concentration respectively, D the thermal molecular diffusivity, k_0 is the constant measures the rate of reaction, σ is the electrical conductivity, c_p is the specific heat at constant pressure, k is the thermal conductivity, T_{∞} and ρ_{∞} are the free stream temperature and density and n be the order of reaction.

The boundary conditions to the present problem can be written as

$$u = bx, \quad v = w = 0, \quad T = T_w, \quad C = C_w \quad \text{at} \quad y = 0 \quad (11)$$

$$u \rightarrow 0, \quad w \rightarrow 0, \quad T \rightarrow T_{\infty}, \quad C \rightarrow C_{\infty} \quad \text{as} \quad y \rightarrow \infty \quad (12)$$

where $b(> 0)$ being stretching rate of the sheet. The boundary conditions on velocity in (11) are the no-slip condition at the surface $y = 0$, while the boundary conditions on velocity at $y \rightarrow \infty$ follow from the fact that there is no flow far way from the stretching surface.

To examine the flow regime adjacent to the sheet, the following transformations are invoked

$$u = bx f'(\eta); \quad v = -\sqrt{b\nu} f(\eta); \quad w = bx g(\eta); \quad \eta = \sqrt{\frac{b}{\nu}} y; \quad \theta(\eta) = \frac{T - T_{\infty}}{T_w - T_{\infty}}; \quad \phi(\eta) = \frac{C - C_{\infty}}{C_w - C_{\infty}} \quad (13)$$

where f is a dimensionless stream function, η is the similarity space variable, θ and ϕ are the dimensionless temperature and concentration respectively. Clearly, the continuity equation (6) is satisfied by u and v defined in (13) on substitution which into equations (7) - (10) gives

$$\begin{aligned} \left(\frac{\theta - \theta_r}{\theta_r}\right) (f'^2 - f f'') + f''' - \left(\frac{\theta'}{\theta - \theta_r}\right) f'' - \left(\frac{\theta - \theta_r}{\theta_r}\right) (Gr\theta + Gc\phi) \\ + M \left(\frac{\theta - \theta_r}{\theta_r}\right) \left(\frac{f' + mg}{1 + m^2}\right) = 0, \end{aligned} \quad (14)$$

$$\left(\frac{\theta - \theta_r}{\theta_r}\right) (f'g - f g') + g'' - \left(\frac{\theta'}{\theta - \theta_r}\right) g' - M \left(\frac{\theta - \theta_r}{\theta_r}\right) \left(\frac{mf' - g}{1 + m^2}\right) = 0, \quad (15)$$

$$(3Nr + 4)\theta'' + 3NrPrf\theta' + 3NrPr\lambda\theta = 0, \quad (16)$$

$$\phi'' + Sc(f\phi' - \gamma\phi^n) = 0, \quad (17)$$

and the transformed boundary conditions are given by

$$f'(\eta) = 1, \quad f(\eta) = 0, \quad g(\eta) = 0, \quad \theta(\eta) = 1, \quad \phi(\eta) = 1 \quad \text{at } \eta = 0, \quad (18)$$

$$f'(\eta) = 0, \quad g(\eta) = 0, \quad \theta(\eta) = 0, \quad \phi(\eta) = 0 \quad \text{at } \eta \rightarrow \infty, \quad (19)$$

where primes denotes differentiation with respect to η only and the dimensionless parameters appearing in the equations (14)-(17) are respectively $\theta_r = \frac{T_r - T_\infty}{T_w - T_\infty} = -\left[\frac{1}{\gamma(T_w - T_\infty)}\right]$ is known as the viscosity parameter, $M = \frac{\sigma B_0^2}{\rho_\infty b}$ the magnetic parameter, $Pr = \frac{\rho_\infty C_p \nu}{k}$ the Prandtl number, $m = \frac{\sigma B_0}{en_e}$ is the Hall current parameter, $\gamma = \frac{k_0}{b} (C_w - C_\infty)^{n-1}$ the non-dimensional chemical reaction parameter, $Gr = \frac{\rho_\infty g \beta_t (T_w - T_\infty)}{b^2 x}$ the Grashof number, $G_c = \frac{\rho_\infty g \beta_c (C_w - C_\infty)}{b^2 x}$ the modified Grashof number, $Nr = \frac{kK}{4T_\infty^3 \sigma^*}$ the thermal radiation parameter, $Sc = \frac{\mu}{\rho_\infty D}$ the Schmidt number and $\lambda = \frac{Q}{\rho_\infty C_p b}$ is defined as the heat generation/absorption parameter.

The important characteristics of the present investigation are the local skin-friction coefficient C_f , the local Nusselt number Nu and the local Sherwood number Sh defined by

$$C_f = \frac{\tau_w}{\mu b x \sqrt{\frac{b}{\nu}}} = f''(0), \quad \text{where } \tau_w = \mu \left(\frac{\partial u}{\partial y}\right)_{y=0} = \mu b x \sqrt{\frac{b}{\nu}} f''(0), \quad (20)$$

$$Nu = \frac{q_w}{k\sqrt{\frac{b}{\nu}}(T_w - T_\infty)} = -\theta'(0), \quad \text{where } q_w = -k\left(\frac{\partial T}{\partial y}\right)_{y=0} = -k\sqrt{\frac{b}{\nu}}(T_w - T_\infty)\theta'(0), \quad (21)$$

$$Sh = \frac{m_w}{D\sqrt{\frac{b}{\nu}}(C_w - C_\infty)} = -\phi'(0), \quad \text{where } m_w = -D\left(\frac{\partial C}{\partial y}\right)_{y=0} = -D\sqrt{\frac{b}{\nu}}(C_w - C_\infty)\phi'(0), \quad (22)$$

If we consider $M = m = 0$ and $Nr = Sc = Gr = Gc = 0$, the present flow problem becomes hydrodynamics boundary-layer flow past a stretching sheet whose analytical solution put forwarded by Crane [2] as follows :

$$f(\eta) = 1 - e^{-\eta} \quad \text{i.e.,} \quad f'(\eta) = e^{-\eta} \quad (23)$$

An attempt has been made to validate our results for the axial velocity $f'(\eta)$, we compared our results with this analytical solution and have found excellent agreement.

3 Numerical Results and Discussion

The system of coupled and non-linear ordinary differential equations (14)-(17) along with the boundary conditions (18) and (19) have been solved numerically by employing a finite difference scheme. We used Newton's linearization method (cf. Cebeci and Couteix [42]) to linearize the discretized equations. The essential features of this technique is that it is based on a finite difference scheme, which has better stability, simple, accurate and more efficient. Finite difference technique leads to a system which is tri-diagonal and therefore speedy convergence as well as economical memory space to store the coefficients. The computational work has been carried out by taking $\delta\eta = 0.0125$ and further reduction in $\delta\eta$ does not bring about any significant change. In the present study, the numerical values to the physical parameters have been chosen so that $M, m, Nr, \theta_r, Pr, Gr, Gc, Sc, n, \gamma$ and λ are varied over a range, which are listed in the figure legends. Fig. 2 shows that our numerical results are complete agreement with those of Crane [2].

Figs. 3 - 10 illustrate the variation of axial velocity for different values of the dimensionless parameters that involved in the present study. Fig. 3 shows that the axial velocity decreases with the increase of the magnetic parameter M , whereas from Fig. 4 it indicates that the axial velocity increases with the increase of Hall parameters m . This is due to the fact that as M increases, the Lorentz force which opposes the flow and leads to deceleration of the fluid motion. By contrast, the cross flow velocity component $g(\eta)$ induced due to Hall effects and shows a anomalous behaviour in $f'(\eta)$ with the variation of M . It has been shown in Figs 5 and 6 that the axial velocity decreases with the increase of the Prandtl number Pr as well as the thermal radiation parameter Nr . This is due to fact that there would be a decrease of boundary-layer thickness in the presence of thermal radiation. Fig. 7 depicts that the axial velocity $f'(\eta)$ increases with the decreasing of the viscosity parameter θ_r . This observation leads to an increase of the thermal boundary-layer thickness. The effects of heat generation parameter ($\lambda > 0$) and absorption parameter ($\lambda < 0$) on the axial velocity displayed in Fig. 8. This figure shows that the axial velocity decreases as the parameter λ increases. The variation of Schmidt number Sc and the chemical reaction parameter γ on the axial velocity profile $f'(\eta)$ shown in Figs. 9 and 10 respectively. It is obvious that the increased values of Sc and γ tend to decreasing of the velocity profiles across the boundary-layer.

Figs. 11 -19 give the distribution of the z - component of velocity, which is induced due to the presence of Hall effects. All these figures show that for any particular values of the physical parameters $g(\eta)$ reaches a maximum value at a certain height η above the sheet and beyond which $g(\eta)$ decreases gradually in asymptotic nature. It is noticed from Fig. 11 is that in the absence of magnetic parameter $M(= 0)$ cross flow velocity vanishes. This is due to fact that, when there is no applied magnetic field, the cross flow velocity would not arise. The variation of Hall current parameter m on the cross-flow velocity $g(\eta)$ shown in Fig. 12. An interesting result observed from this figure that the cross-flow velocity gradually increases with the increase of $m \leq 2$ and the velocity decreases for $m > 2$. The values of m beyond which the flow behaviour changes is considerable depend upon the choice of the magnetic parameter M . Thus we conclude that after certain magnetic field strength the flow behaviour is significantly affected. Figs. 13 and 14 indicate that the cross-flow velocity $g(\eta)$ decreases with increasing the Prandtl number Pr and the thermal radiation parameter Nr , while from Fig. 15 that the trend is reversed after

a certain height above the sheet. This is lies in the fact that the increase of Prandtl number Pr and the thermal radiation Nr give rise to decrease of the momentum boundary-layer thickness. We observed from Figs. 16, 17 and 19 that the cross-flow velocity decreases with the increase of the heat generation/absorption parameter λ , Schmidt number Sc and the chemical reaction parameter γ . However, the cross-flow velocity increases as the order of the chemical reaction n increases.

The distribution of dimensionless temperature $\theta(\eta)$ along the height of the stretching sheet for different values of the dimensionless parameters involved in the present study displayed through Figs. 20 - 25. Fig. 20 shows that by the application of an external magnetic enhances the temperature of the fluid, while the effect of the Hall current parameter m has an reducing effect on the dimensionless temperature $\theta(\eta)$ shown in Fig. 21. It may note that the effect of Hall current parameter m opposes the effect of magnetic field on the temperature distribution. Fig. 22 presents the variation of Prandtl number Pr on the temperature $\theta(\eta)$. The results presented in Fig. 22 shows that the dimensionless temperature decreases as the Prandatl number Pr increases. This is lies in the fact that smaller values of Pr are equivalent to increasing of thermal conductivities and therefore heat is able diffuse away from the stretching sheet. Fig. 23 represents the temperature profiles for various values of the thermal radiation parameter Nr in the boundary-layer. Increasing the thermal radiation parameter Nr produces a decrease in the temperature of the fluid. This is because of the fact that the thermal boundary-layer thickness decreases with increasing the thermal radiation parameter. Fig. 24 gives the variation of the viscosity parameter θ_r on the temperature profiles and which shows that no significant change occur with the increase of the values of θ_r . It is evident that the energy equation (16) is uncoupled from the viscosity parameter θ_r . For this reason no figures are presented herein for the variation of Sc , n and γ . The effect of heat generation/absorption parameter λ on the dimensionless temperature $\theta(\eta)$ is shown in Fig. 25. It is clear that an increase in the heat generation/absorption parameter λ leads to a decrease of $\theta(\eta)$. Thus the effect of internal heat generation is to decrease the rate of energy transport to the fluid, thereby decreasing the temperature of the fluid.

The effect of the imposition of various parameters on concentration profiles are shown in

Figs. 26 - 31. It is observed from Figs. 26 and 27 that under the action of a strong magnetic field, the concentration species has an enhancing effect, whereas it has the reducing effect on the Hall current parameter m . The reason behind this is that in equations (14) and (15), the parameters M and m are connected by the relations of the form $\frac{M}{1+m^2}$ and $\frac{Mm}{1+m^2}$. As the variation of concentration profiles for different values of the parameters Nr and θ_r agrees with the temperature profiles, we do not have presented those results. However, Fig. 28 is the variation of heat generation/absorption parameter λ on the species concentration, which opposes the variation of the temperature distribution. Fig. 29 depicts the variation of Schmidt number Sc on the species concentration $\phi(\eta)$. It is observed that the species concentration decreases with the increase of the Schmidt number Sc . Physically, which shows that the increase of Sc causes decrease of molecular diffusion D . The influence of chemical reaction parameter γ on the species concentration profiles for generative chemical reaction is shown in Fig. 30. It is noticed that the increasing values of the chemical reaction parameter γ is to decelerate the concentration distribution in the boundary-layer. This is due to fact that destructive ($\gamma > 0$) chemical reaction decreases the shortest boundary-layer thickness and thereby increasing the species concentration. It is observed from Fig. 31 that the increasing effect of the order of chemical reaction parameter n is to enhances the mass transfer in the boundary-layer.

The problems of engineering interest for the present study are the local skin-friction coefficient C_f , the local Nusselt number Nu and the local sherwood number Sh which indicates physically the wall shear stress, the rate of heat transfer at the sheet and the rate of mass transfer respectively. The expressions of these physical quantities have been presented in equations (20)- (22). Tables 1-3 exhibit the numerical values to the local skin-friction coefficient $f''(0)$, the local Nusselt number $-\theta'(0)$ and the local sherwood number $-\phi'(0)$ respectively. It has been observed that for any particular values of the parameters Pr , Nr , m , θ_r , γ , λ and Sc , the local skin-friction coefficient, the local Nusselt number and the local Shearwood number decreases with the increase of the magnetic parameter M . Table -1 shows that for fixed value of M , the local skin-friction C_f decreases with increasing the values of the Prandatl number Pr , thermal radiation parameter Nr , viscosity parameter θ_r , the rate of chemical reaction γ , heat generation/absorption parameter λ and the Schmidt number Sc . Physically, we meant that for the increasing of the thermal radiation parameter Nr leads to decreasing in the boundary-layer

thickness. However, the skin-friction coefficient increases as the Hall parameter m increases. It is worthwhile to observed from Table-2 that the rate of heat transfer at the sheet increases with the increase of the parameters Pr , Nr , m and γ . The increase of the thermal radiation parameter Nr has an enhancing effect on the thermal boundary-layer thickness. It is also noticed that the increasing of the parameters θ_r , γ and Sc is to reduce the heat transfer rate and which shows that the rate of change of heat transfer is insignificant. The rate of mass transfer increases significantly when the Hall parameter m , the chemical reaction parameter γ and the Schmidt number Sc increases. Moreover, the rate of mass transfer decreases insignificantly with the increase of the parameters Pr , Nr and λ .

4 Conclusions

In the present investigation, we dealt with the combined effects of thermal radiation and Hall current on the boundary-layer fluid flow, heat and mass transfer with temperature dependent viscosity. The highly non-linear coupled system of partial differential equations characterizing the flow, heat and mass transfer has been reduced to a coupled system of non-linear ordinary differential equations by applying a suitable similarity transformations. The resulting system solved numerically by using the finite difference scheme along with the Newton's linearization technique. The obtained numerical results have been presented through the figures and in tabular form to illustrate the details of the flow behaviour, heat and mass transfer phenomena and their dependence on the physical parameters that involved in the present investigation. From our computed numerical results we observed that the magnetic field and Hall current produce opposite effects on the velocity distribution and heat transfer as well as on the concentration distribution. For a fixed value of M , the skin-friction increases with an increase in m and similar is the observation for heat and mass transfer rate. Sufficiently strong heat generation parameter may alter the temperature gradient. Temperature decreases and the concentration increases with increasing values of Prandtl number Pr . But a reversal trend is observed when the values of the thermal radiation parameter increases. The species concentration decreases with an increase in the values of the Schmidt number Sc and chemical reaction parameter λ whereas opposite trend is observed in the case of the order of the chemical reaction. It is hoped that

the results obtained will serve as a scientific tool for understanding more complex flow problems and provide more useful information for engineering applications.

References

- [1] Sakiadis BC. Boundary layer behavior on continuous solid surfaces. Am. Inst. Chem. Engg. J. (AIChE) 7(1961) 26-28.
- [2] Crane LJ. : Flow past a stretching sheet. Z. Angew. Math. Phys. (ZAMP), 21(1970) 645-647.
- [3] Rajagopal KR, Na TY and Gupta AS. Flow of a viscoelastic fluid over a stretching sheet. Rheol. Acta, 23(1984) 213-215.
- [4] Wang CY. Non-linear stretching due to the oscillatory stretching of a sheet in a viscous fluid. Acta Mech. 72 (1988) 261-268.
- [5] Soundalgekar VM and Gupta SK. Free convection effects on the oscillatory flow of a viscous, incompressible fluid past a steadily moving vertical plate with constant suction. Int. J. Heat Mass Transf. 18(1975) 1083-1093.
- [6] Cortell R. A note on magnetohydrodynamic flow of a power-law fluid over a stretching sheet. Appl. Math. Comput. 168 (2005) 557-566.
- [7] Dandapat BS and Gupta AS. Flow and heat transfer in a viscoelastic fluid over a stretching sheet. Int. J. Non-linear Mech. 24 (1989) 215-219.
- [8] Rajagopal KR, Na TY and Gupta AS. A non-similar boundary layer flow on a stretching sheet in a non-Newtonian fluid with uniform free stream. J. Math. Phys. Sci. 21 (1987) 189-200.
- [9] Mahapatra TR and Gupta AS. Heat transfer in stagnation-point flow towards a stretching sheet, Heat Mass Transf. 38 (2002) 517-523.
- [10] Danberg JE and Fansler KS. A non-similar moving wall boundary layer problem. Quart. Appl. Math. 34 (1974) 305-309.
- [11] Gupta PS and Gupta AS. Heat and Mass Transfer on a stretching sheet with suction or blowing. Cand. J. Chem. Engg. 55 (1977) 744-746.
- [12] Pavlov KB. Magnetohydrodynamic flow of an incompressible viscous fluid caused by deformation of plane surface. Magnitnaya Gidrodinamika, 4 (1974) 146-147.

- [13] Andersson HI. MHD flow of a visco-elastic fluid past a stretching surface. *Acta Mech.* 95 (1992) 227-230.
- [14] Andersson HI, Bech KH and Dandapat BS. Magnetohydrodynamic flow of a Power-law fluid over a stretching surface. *Int. J. Non-Linear Mech.* 27 (1992) 929-936.
- [15] Chakrabarty A and Gupta AS. Hydromagnetic flow of heat and mass transfer over a stretching sheet. *Quart. Appl. Math* 33 (1979) 73-78.
- [16] Char MI. Heat transfer in a hydromagnetic flow over a stretching sheet. *Heat and Mass Transf.* 29 (1994) 495-500.
- [17] Watanabe T and Pop I. Magnetohydrodynamics free-convection flow over a wedge in the presence of a transverse magnetic field. *Int. Commun. Heat and Mass transf.* 20 (1993) 871-881.
- [18] Elbashbeshy EMA. Heat and Mass transfer along a vertical plate with variable surface tension and concentration in the presence of the magnetic field. *Int. J. Eng. Sci.* 35 (1997) 515-522.
- [19] Afify AA. MHD free-convective flow and mass transfer over a stretching sheet with chemical reaction. *Heat Mass Transf.* 40 (2004) 495-500.
- [20] Watanabe T and Pop I. Hall effects on magnetohydrodynamic boundary layer flow over a continuous moving flat plate. *Acta Mech.* 108 (1995) 35-47.
- [21] Aboeldahab EM. Hall effects on magnetohydrodynamic free-convective flow at a stretching surface with a uniform free stream. *Physica Scripta.* 63 (2001) 29-35.
- [22] Aboeldahab EM and Elbarbary EME. Hall current effect on magnetohydrodynamic free-convection flow past a semi-infinite vertical plate with mass transf. *Int. J. Eng. Sci.* 39 (2001) 1641-1652.
- [23] Shit GC. Hall effects on MHD free-convective flow and mass transfer over a stretching sheet. *Int. J. Appl. Math. Mech.(IJAMM)* in press (2009).
- [24] Fakhar K. Hall effects on Unsteady Magnetohydrodynamic flow of a third grade fluid. *Chin. Phys. Lett.* 24 (2007) 1129-1132.
- [25] Rana MA, Siddiqui AM and Ahmed N. Hall effect on Hartmann flow and heat transfer of a Burger's fluid. *Phys. Letters A,* 372 (2008) 562-568.
- [26] Raptis A and Perdikis C. Viscoelastic flow by the presence of radiation. *ZAMM.* 78 (1998) 277-279.
- [27] Rapits A. Flow of a micropolar fluid past a continuously moving plate by the presence of radiation. *Int. J. Heat mass transf.* 41 (1998) 2865-2866.

- [28] Mukhopadhaya S, Layek GC and Samad A. Study of MHD boundary layer flow over a heated stretching sheet with variable viscosity. *Int. J. Heat Mass Transf.* 48 (2005) 4460-4466.
- [29] Shateyi S. Thermal radiation and bouyancy effects on heat and mass transfer over a semi-infinite stretching surface with suction and blowing. *J. Appl. Math.* volume 2008, Article ID 414830 , 12 pages.
- [30] Mahmoud MAA. Thermal radiation effect on unsteady MHD free convection flow past a vertical plate with temperature-dependent viscosity. *Cand. J. Chem. Eng* vol-87 (2009) 47-52.
- [31] Pal D and Talukder B. Perturbation analysis of unsteady magnetohydrodynamic convective heat and mass transfer in a boundary-layer slip flow past a vertical permeable plate with thermal radiation and chemical reaction. *Commun. Non-linear. Sci. Numer Simulat.* (2009), doi : 10.1016/j.cnsns .2009.07.011
- [32] Pal D and Chatterjee S. Heat and mass transfer in MHD non-Darcian flow of a micropolar fluid over a stretching sheet embedded in a porous media with non-uniform heat source and thermal radiation. *Commun. Non-linear Sci. Numer. Simulat.*(2009), doi: 10.1016/j.cnsns.2009.07.024
- [33] Salem AM. Variable viscosity and thermal conductivity effects on MHD flow and heat transfer in viscoelastic fluid over a stretching sheet. *Physics Letters A* 369 (2007) 315-322.
- [34] Shit GC and Haldar R. Effect of thermal radiation on MHD viscoelastic fluid flow over a stretching sheet with variable viscosity, Communicated for publication in *Int. J. Fluid Mech. Res* (2009).
- [35] Muthucumarswamy R and Ganesan P. Effect of the chemical reaction and injection on flow characteristics in an unsteady upward motion of an isothermal plate, *J. Appl. Mech. Tech. Phys.* 42 (2001) 665-671.
- [36] Chamakha AJ. MHD flow of a uniformly stretched vertical permeable surface in the presence of heat generation/absorption and a chemical reaction, *Int. Commun. Heat mass transf.* 30 (2003) 413-422.
- [37] Mohamed RA and Abo-Dahab SM. Influence of chemical reaction and thermal radiation on the heat and mass transfer in MHD micropolar flow over a vertical moving porous plate in a porous medium with heat generation. *Int. J. Thermal Sciences.* 48 (2009) 1800-1813.
- [38] Seddeek MA, Darwish AA and Abdelmeguid MS. Effects of chemical reaction and variable viscosity on hydromagnetic mixed convection heat and mass transfer for Hiemenz flow through porous media with radiation. *Commun. Non-linear Sci. Numer. Simulat.* 12 (2007) 195-213.

- [39] Sedeek MA. Thermal radiation and bouyancy effects on MHD free convective heat generation flow over an acceleracting permeable surface with temperature dependent viscosity. *Cand. J. Phys.* 79 (2001) 725 - 732.
- [40] Cowling TG (1957) *Magnetohydrodynamics*, Interscience Publishers, New York.
- [41] Lai FC and Kulacki FA. The effect of variable viscosity on convective heat transfer along a vertical surface in a saturated porous medium. *Int. J. Heat Mass Transf.* 33 (1990) 1028-1031.
- [42] Cebeci T, Cousteix J. *Modeling and computation of boundary-layer flows*. Springer-Verlag 1999.

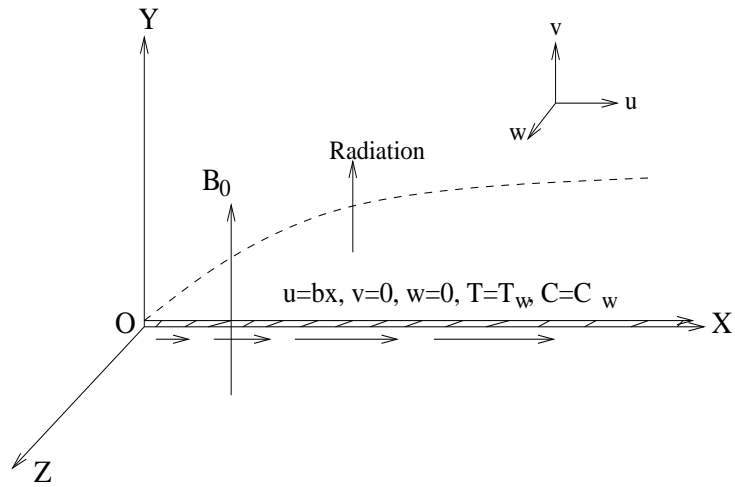


Fig. 1 Physical sketch of the problem

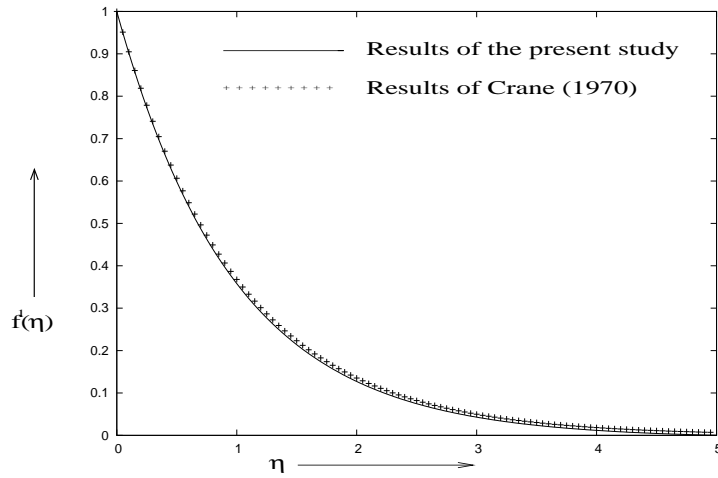


Fig. 2 Comparison of axial velocity profile $f'(\eta)$ with the results of Crane [2] for $M = Gr = Gc = Sc = Pr = Nr = 0.0$

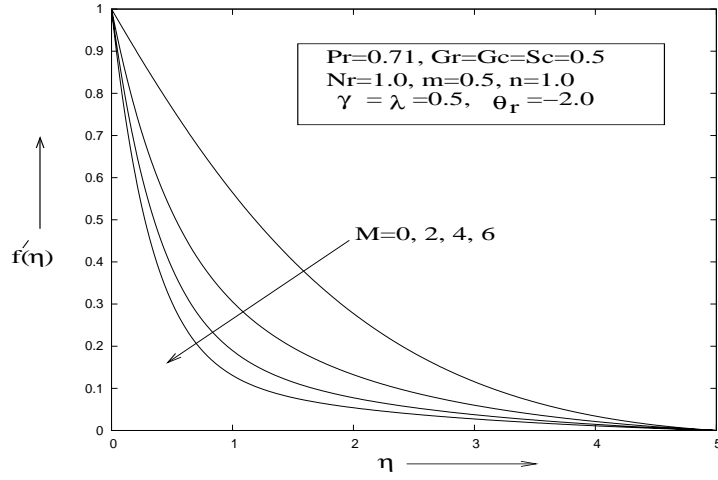


Fig. 3 Variation of $f'(\eta)$ with η for different values of M

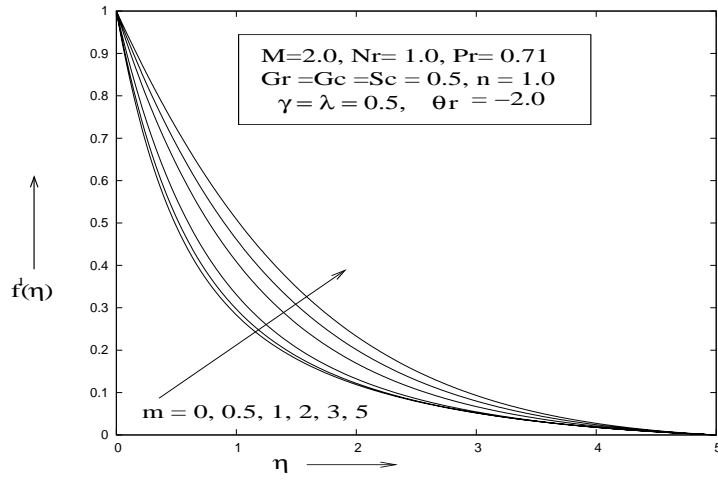


Fig. 4 Variation of $f'(\eta)$ with η for different values of m

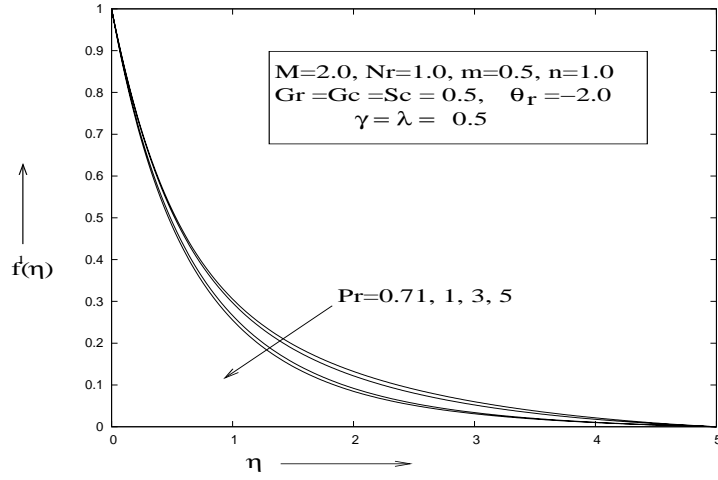


Fig. 5 Variation of $f'(\eta)$ with η for different values of Pr

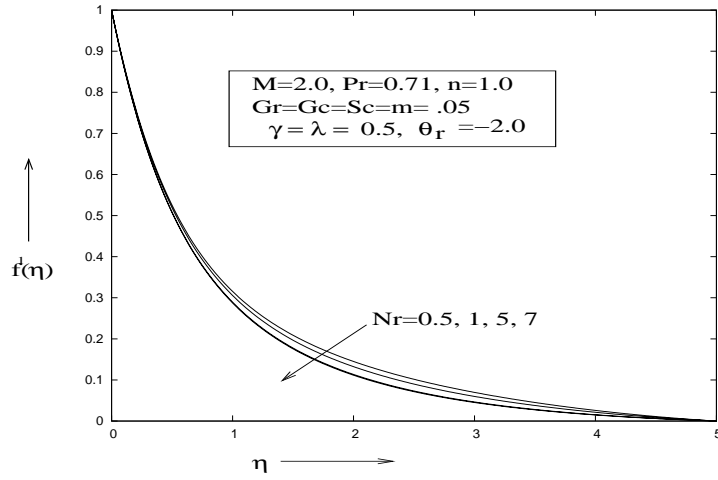


Fig. 6 Variation of $f'(\eta)$ with η for different values of Nr

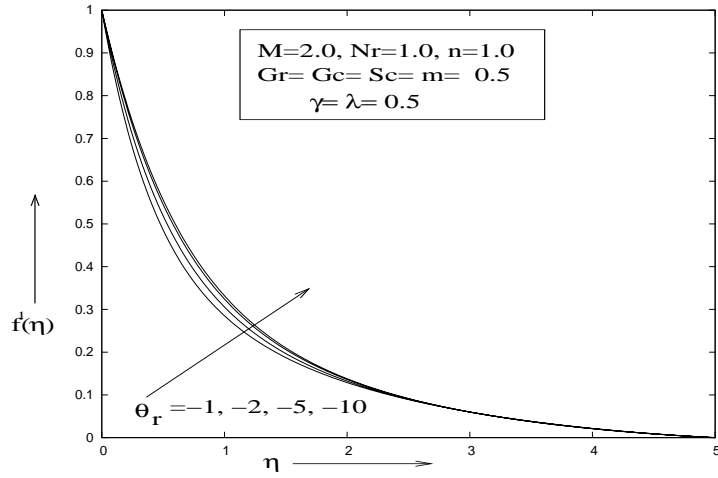


Fig. 7 Variation of $f'(\eta)$ with η for different values of θ_r .

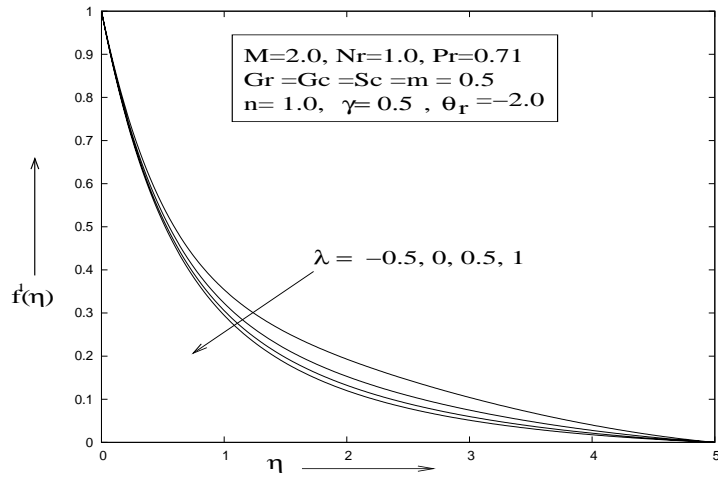


Fig. 8 Variation of $f'(\eta)$ with η for different values of λ .

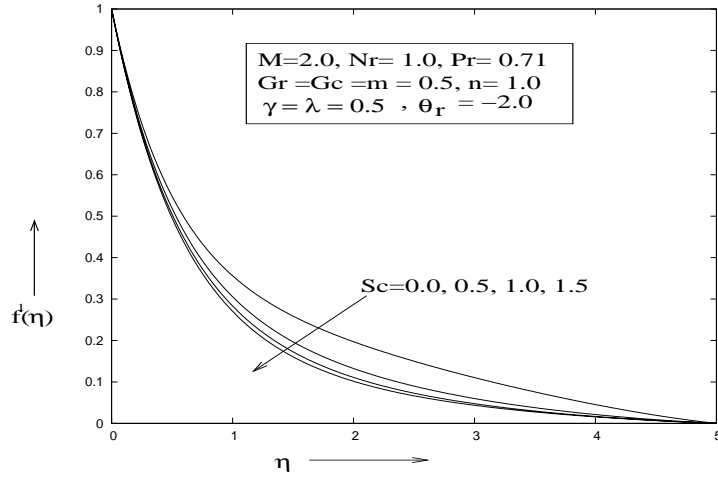


Fig. 9 Variation of $f'(\eta)$ with η for different values of Sc

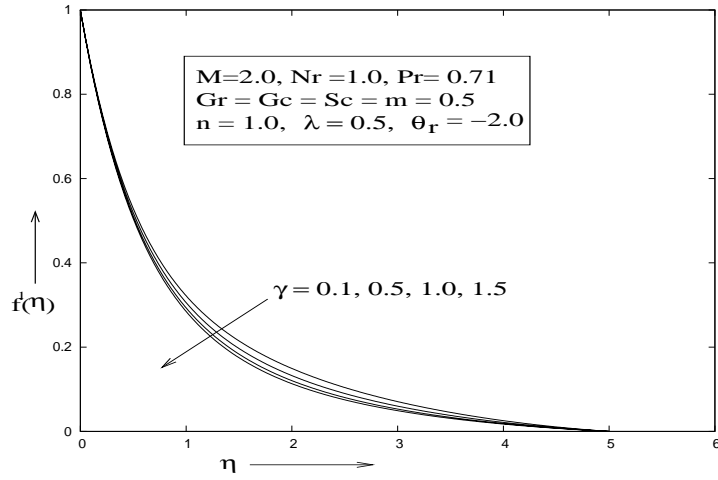


Fig. 10 Variation of $f'(\eta)$ with η for different values of γ

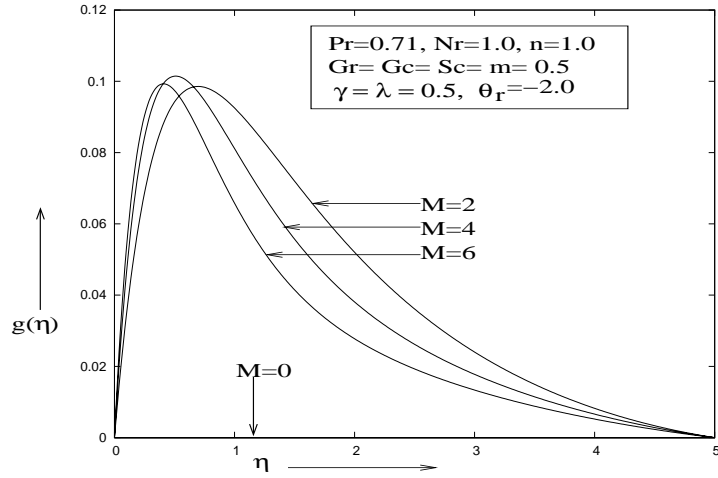


Fig. 11 Variation of $g(\eta)$ with η for different values of M

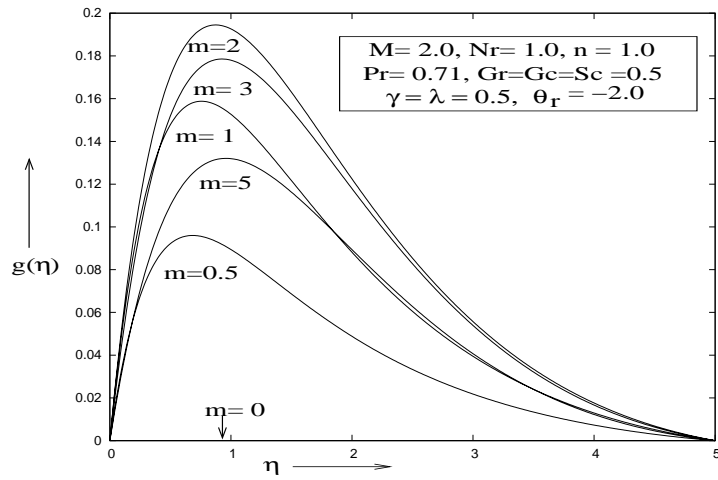


Fig. 12 Variation of $g(\eta)$ for different values of the Hall parameter m .

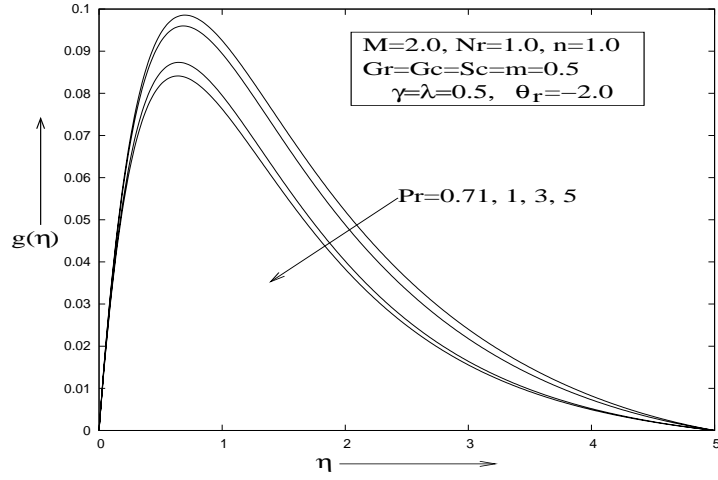


Fig. 13 Variation of $g(\eta)$ with η for different values of Pr

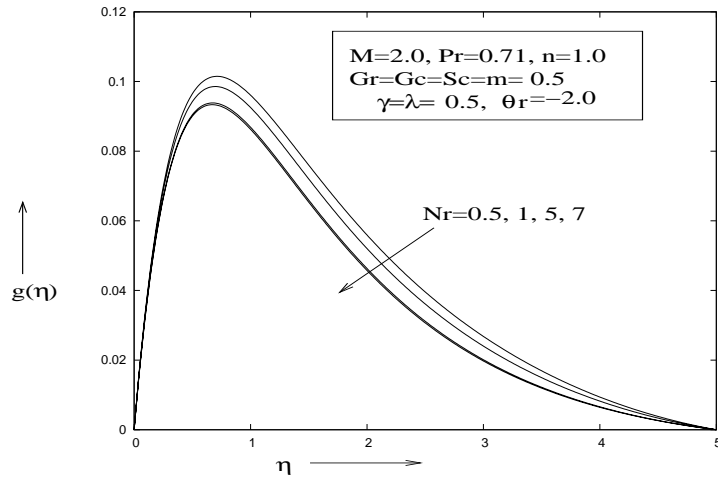


Fig. 14 Variation of $g(\eta)$ with η for different values of Nr

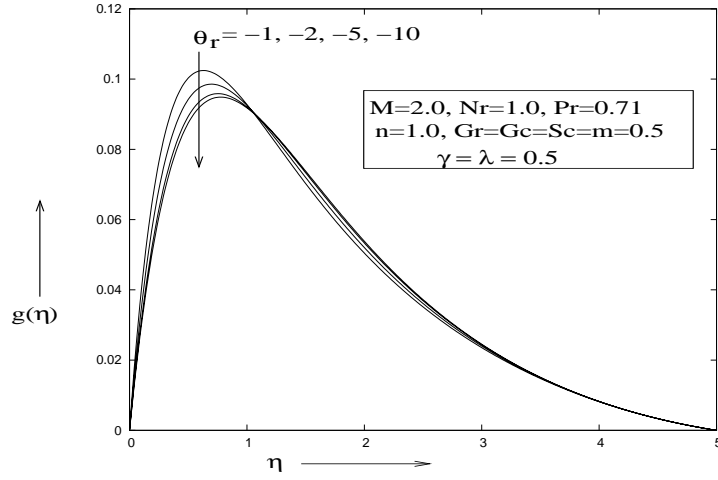


Fig. 15 Variation of $g(\eta)$ with η for different values of θ_r

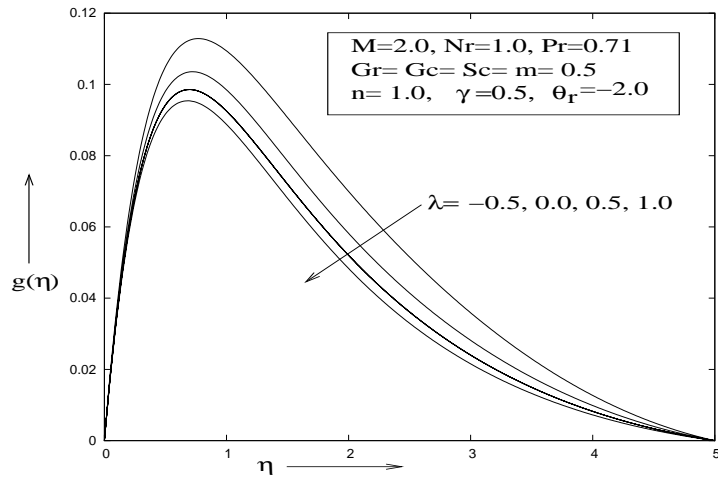


Fig. 16 Variation of $g(\eta)$ with η for different values of λ

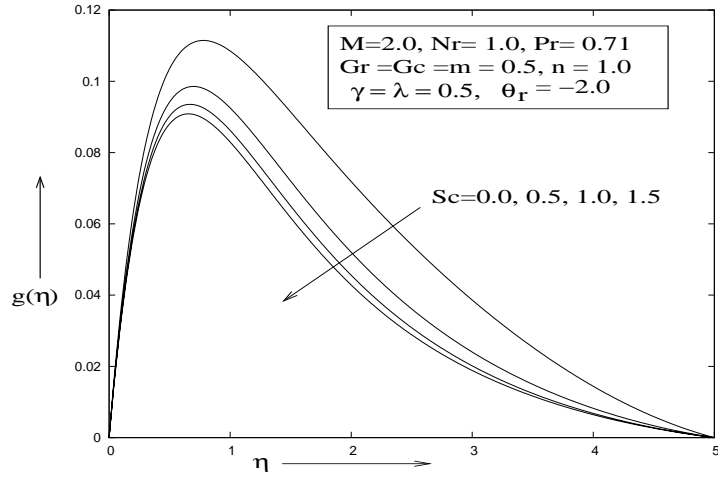


Fig. 17 Variation of $g(\eta)$ with η for different values of Sc

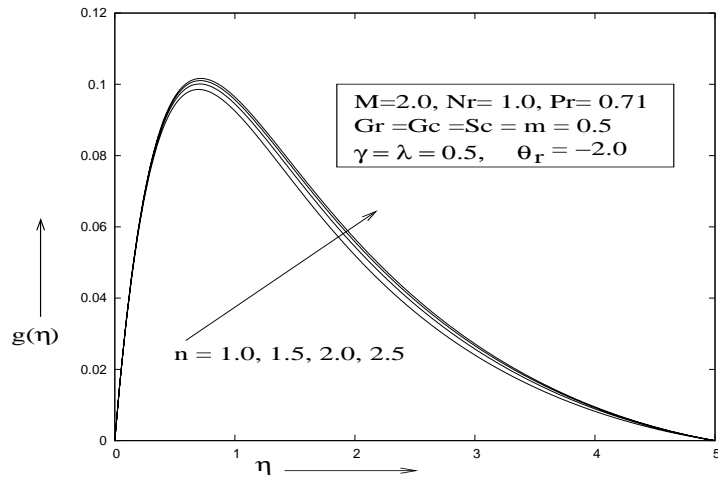


Fig. 18 Variation of $g(\eta)$ with η for different values of n

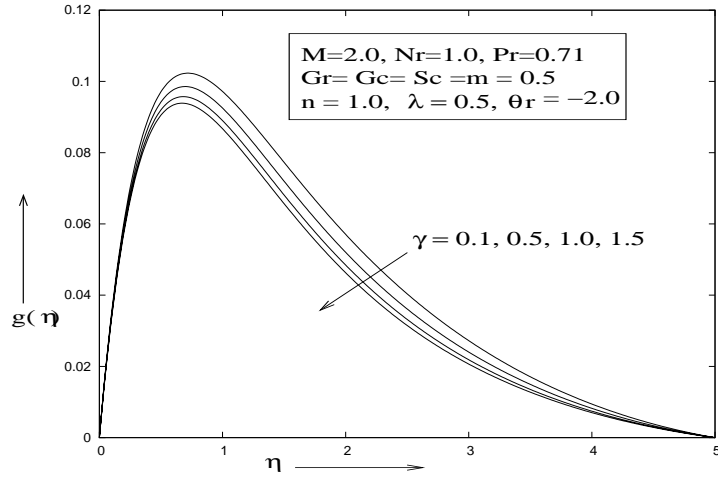


Fig. 19 Variation of $g(\eta)$ with η for different values of γ

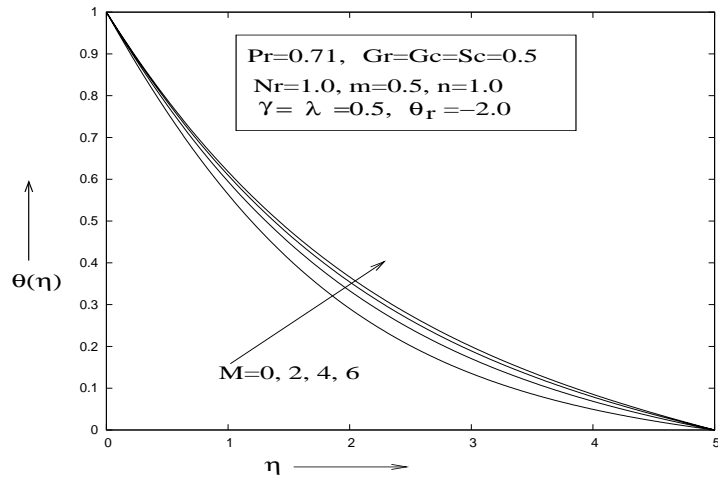


Fig. 20 Distribution of dimensionless temperature $\theta(\eta)$ with η for different values of M

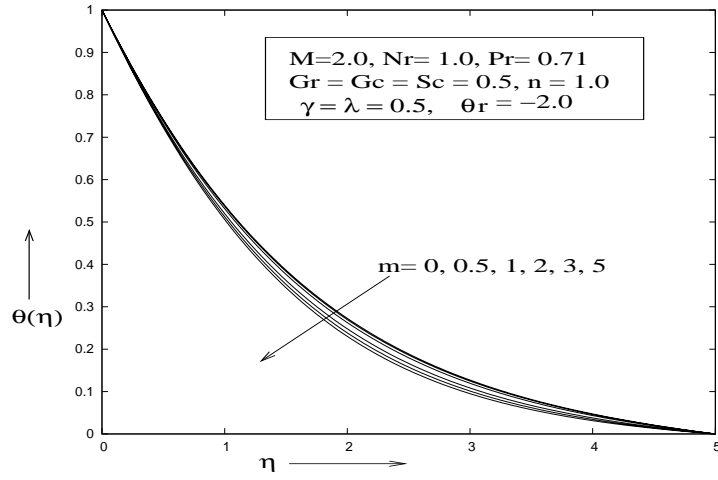


Fig. 21 Distribution of dimensionless temperature $\theta(\eta)$ with η for different values of m

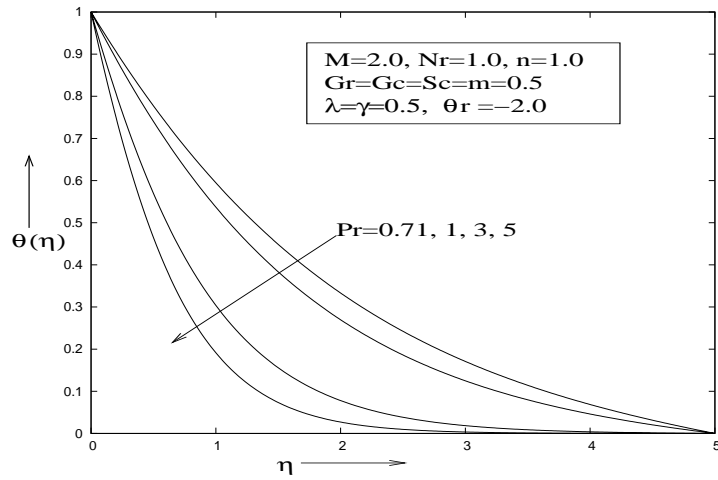


Fig. 22 Distribution of dimensionless temperature $\theta(\eta)$ with η for different values of Pr

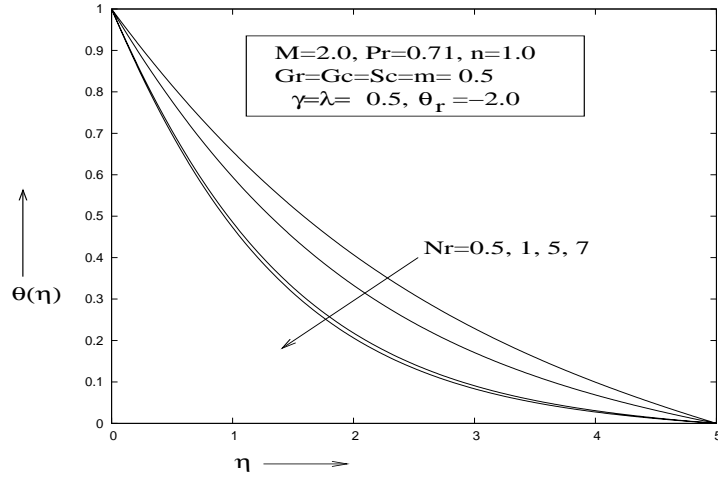


Fig. 23 Distribution of dimensionless temperature $\theta(\eta)$ with η for different values of Nr

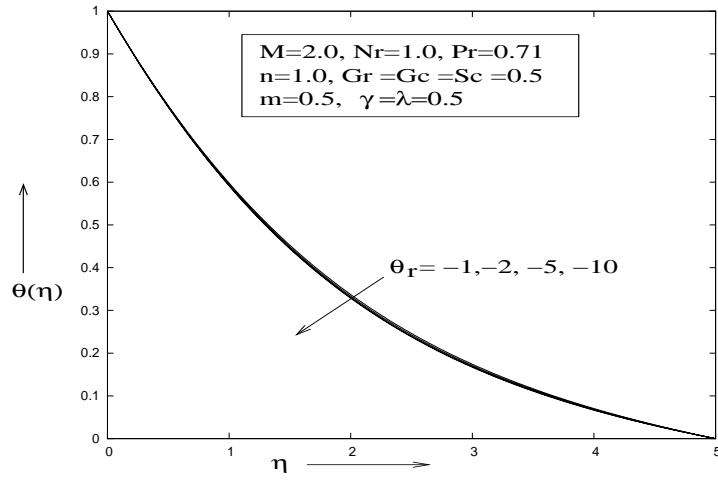


Fig. 24 Distribution of dimensionless temperature $\theta(\eta)$ with η for different values of θ_r

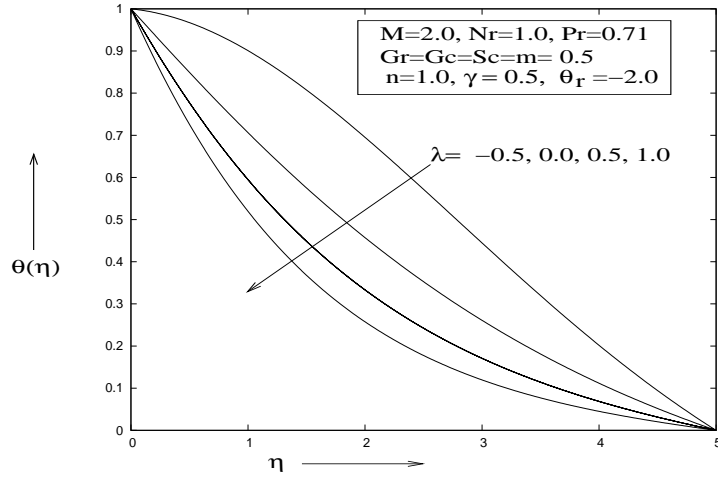


Fig. 25 Distribution of dimensionless temperature $\theta(\eta)$ with η for different values of λ

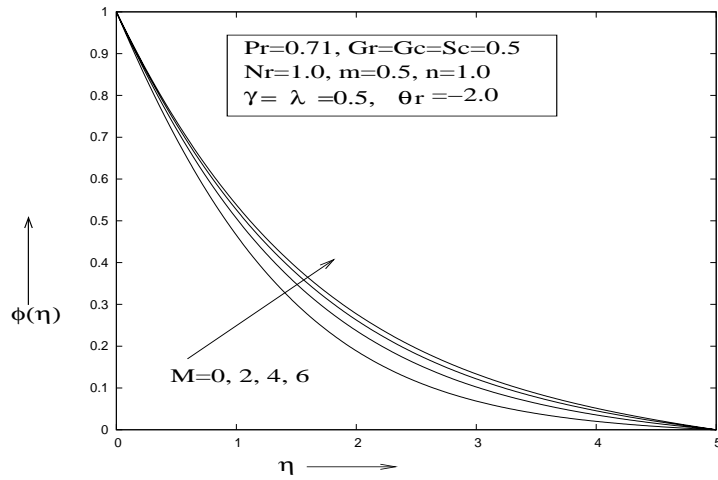


Fig. 26 Influence of concentration species $\phi(\eta)$ with η for different values of M

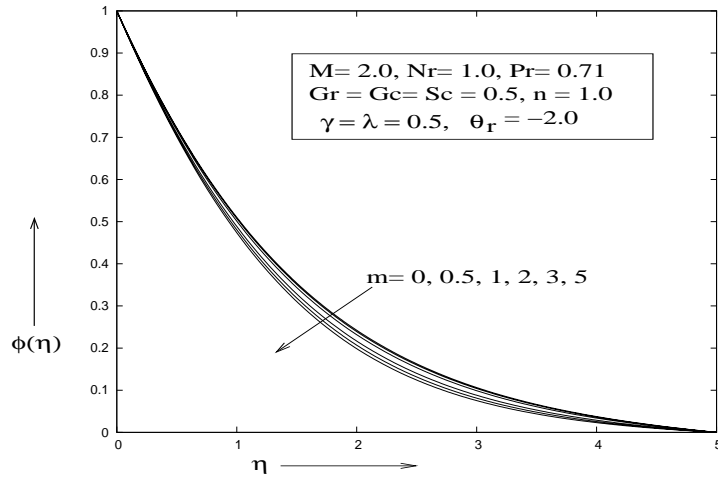


Fig. 27 Influence of concentration species $\phi(\eta)$ with η for different values of m

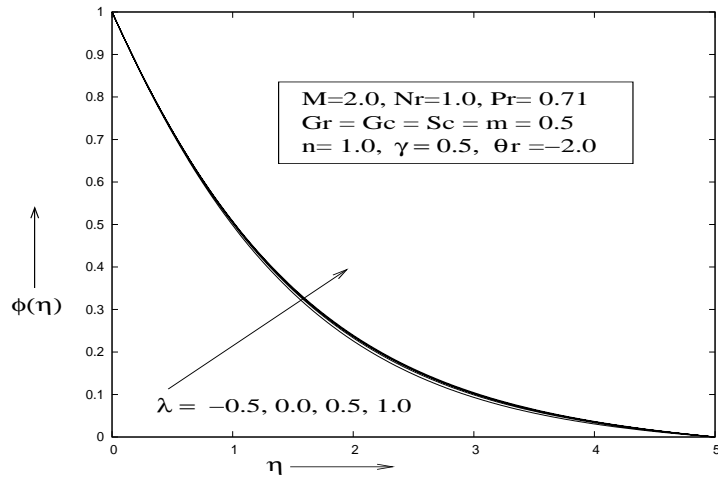


Fig. 28 Influence of concentration species $\phi(\eta)$ with η for different values of λ

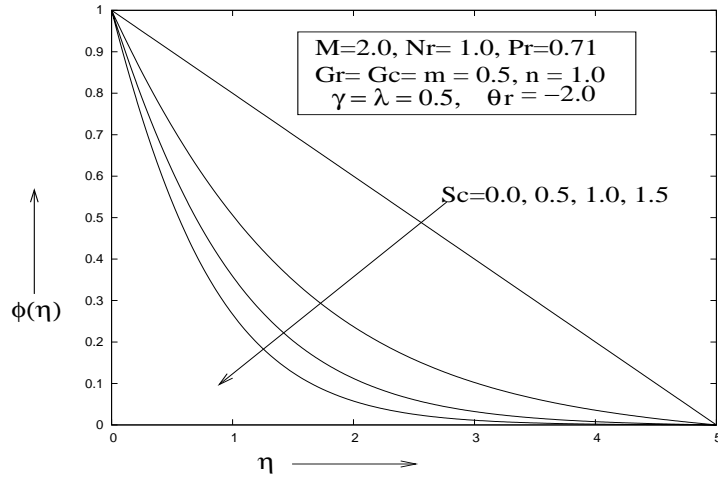


Fig. 29 Influence of concentration species $\phi(\eta)$ with η for different values of Sc

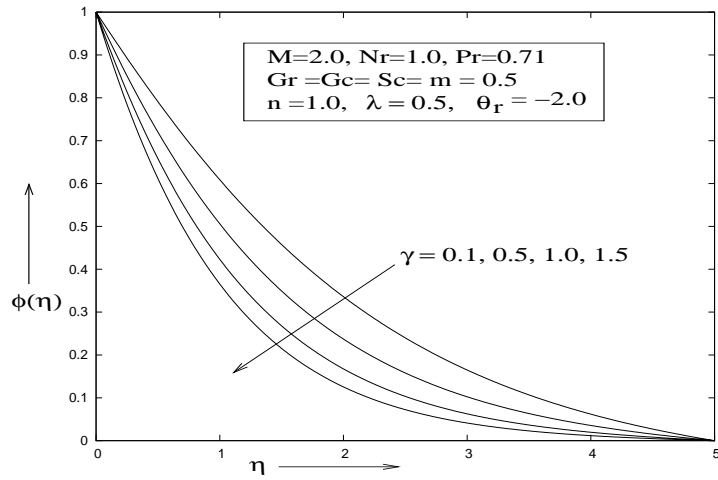


Fig. 30 Influence of concentration species $\phi(\eta)$ with η for different values of γ

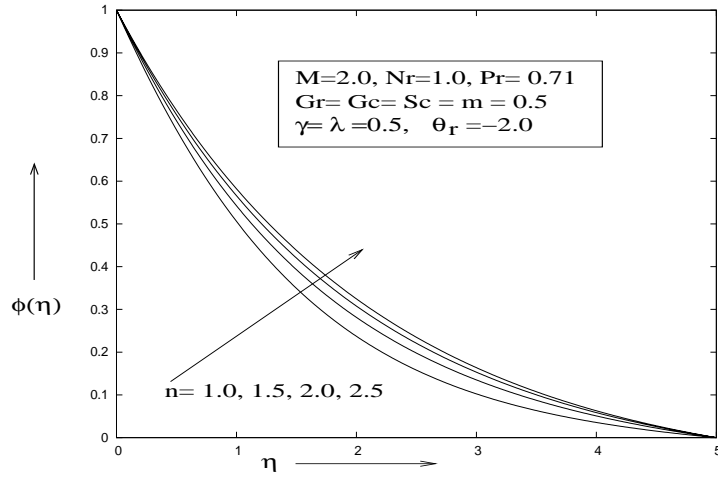


Fig. 31 Influence of concentration species $\phi(\eta)$ with η for different values of n

Table-1. Numerical values of the local skin-friction coefficient $C_f = f''(0)$

Pr	Nr	m	θ_r	γ	λ	Sc	$M = 0.0$	$M = 2.0$	$M = 4.0$
0.71	1.0	0.5	-2.0	0.5	0.5	0.5	-0.52597	-1.45996	-2.10233
	1.0						-0.55356	-1.47541	-2.11350
	3.0						-0.66289	-1.55043	-2.17159
0.71	0.5	0.5	-2.0	0.5	0.5	0.5	-0.49627	-1.44462	-2.09153
	1.0						-0.52596	-1.45996	-2.10233
	5.0						-0.57792	-1.49009	-2.12436
0.71	1.0	1.0	-2.0	0.5	0.5	0.5	-0.52596	-1.22516	-1.76392
		3.0					-0.52596	-0.73786	-1.00484
		5.0					-0.52596	-0.61575	-0.75757
0.71	1.0	0.5	-1.0	0.5	0.5	0.5	-0.56098	-1.66484	-2.41425
			-2.0				-0.52596	-1.45996	-2.10233
			-5.0				-0.49443	-1.31365	-1.88306
0.71	1.0	0.5	-2.0	0.1	0.5	0.5	-0.49746	-1.44034	-2.08909
				0.5			-0.52596	-1.45996	-2.10233
				1.0			-0.55088	-1.47691	-2.11402
0.71	1.0	0.5	-2.0	0.5	-0.5	0.5	-0.42172	-1.38284	-2.04079
					0.0		-0.48498	-1.43029	-0.7862
					0.5		-0.52596	-1.45996	-2.10233
0.71	1.0	0.5	-2.0	0.5	-0.5	0.5	-0.52596	-1.45996	-2.10233
						1.0	-0.57899	-1.48921	-2.12044
						1.5	-0.61068	-1.50989	-2.13432

Table-2. Numerical values of the local Nusselt number $Nu = -\theta'(0)$

Pr	Nr	m	θ_r	γ	λ	Sc	$M = 0.0$	$M = 2.0$	$M = 4.0$
0.71	1.0	0.5	-2.0	0.5	0.5	0.5	0.51857	0.48436	0.46751
	1.0						0.61651	0.57475	0.55368
	3.0						1.09706	1.03107	0.99413
0.71	0.5	0.5	-2.0	0.5	0.5	0.5	0.41891	0.39371	0.38159
	1.0						0.51857	0.48436	0.46751
	5.0						0.70871	0.66088	0.63618
0.71	1.0	1.0	-2.0	0.5	0.5	0.5	0.51857	0.48973	0.47213
		3.0					0.51857	0.50769	0.49279
		5.0					0.51857	0.51382	0.50509
0.71	1.0	0.5	-1.0	0.5	0.5	0.5	0.51673	0.48081	0.46364
			-2.0				0.51857	0.48436	0.46751
			-5.0				0.52016	0.48729	0.47070
0.71	1.0	0.5	-2.0	0.1	0.5	0.5	0.52097	0.48641	0.46901
				0.5			0.51857	0.48436	0.46751
				1.0			0.51662	0.48279	0.46639
0.71	1.0	0.5	-2.0	0.5	-0.5	0.5	0.12334	0.02936	-0.02061
					0.0		0.35575	0.30484	0.27964
					0.5		0.57857	0.48436	0.46751
0.71	1.0	0.5	-2.0	0.5	-0.5	0.5	0.51857	0.48436	0.46751
						1.0	0.51425	0.48156	0.46573
						1.5	0.51223	0.48004	0.46469

Table-3. Numerical values of the local Sherwood number $Sh = -\phi'(0)$

Pr	Nr	m	θ_r	γ	λ	Sc	$M = 0.0$	$M = 2.0$	$M = 4.0$
0.71	1.0	0.5	-2.0	0.5	0.5	0.5	0.67199	0.62481	0.60072
	1.0						0.66905	0.62322	0.59979
	3.0						0.66032	0.61772	0.59634
0.71	0.5	0.5	-2.0	0.5	0.5	0.5	0.67544	0.62659	0.60175
	1.0						0.67199	0.62481	0.60072
	5.0						0.66670	0.62188	0.59898
0.71	1.0	1.0	-2.0	0.5	0.5	0.5	0.67199	0.63256	0.60770
		3.0					0.67199	0.65744	0.63733
		5.0					0.67199	0.66566	0.65406
0.71	1.0	0.5	-1.0	0.5	0.5	0.5	0.66593	0.61956	0.59486
			-2.0				0.67199	0.62481	0.60072
			-5.0				0.67411	0.62911	0.60553
0.71	1.0	0.5	-2.0	0.1	0.5	0.5	0.50642	0.43681	0.40050
				0.5			0.67199	0.62481	0.60072
				1.0			0.83627	0.80234	0.78493
0.71	1.0	0.5	-2.0	0.5	-0.5	0.5	0.68296	0.63338	0.60670
					0.0		0.67616	0.62786	0.60279
					0.5		0.67199	0.62481	0.60072
0.71	1.0	0.5	-2.0	0.5	-0.5	0.5	0.67199	0.62481	0.60072
						1.0	0.96662	0.90329	0.86889
						1.5	1.19569	1.12354	1.08281